BRAF-mutant Transcriptional Subtypes Predict Outcome of Combined BRAF, MEK, and EGFR Blockade with Dabrafenib, Trametinib, and Panitumumab in Patients with Colorectal Cancer

Authors and Affiliations:

Gary Middleton[1], Yiqun Yang[2], Catarina D. Campbell[2], Thierry André[3], Chloe E. Atreya[4], Jan H.M. Schellens[5], Takayuki Yoshino[6], Johanna C. Bendell[7], Antoine Hollebecque[8], Autumn J. McRee[9], Salvatore Siena[10,11], Michael S. Gordon[12], Josep Tabernero[13], Rona Yaeger[14], Peter J. O'Dwyer[15], Filip De Vos[16], Eric Van Cutsem[17], John M. Millholland[2], Jan C. Brase[18], Fatima Rangwala[19], Eduard Gasal[19], Ryan Corcoran[20]

[1]Institute of Immunology and Immunotherapy, University of Birmingham, Birmingham, United Kingdom. [2]Novartis Institutes for BioMedical Research, Cambridge, Massachusetts. [3]Hôpital Saint-Antoine and Sorbonne Universités, UPMC Paris 06, Paris, France. [4]Helen Diller Family Comprehensive Cancer Center, University of California, San Francisco, San Francisco, California. [5]The Netherlands Cancer Institute, Amsterdam, the Netherlands. [6]National Cancer Center Hospital East, Chiba, Japan. [7]Sarah Cannon Research Institute/Tennessee Oncology, Nashville, Tennessee. [8]Institute Gustave Roussy, Villejuif, France. [9]University of North Carolina, Chapel Hill, North Carolina. [10]Department of Oncology and Hemato-Oncology, Università degli Studi di Milano, Milan, Italy. [11]Niguarda Cancer Center, Grande Ospedale Metropolitano Niguarda, Milan, Italy. [12]Pinnacle Oncology Hematology, Scottsdale, Arizona. [13]Vall d'Hebron University Hospital, Barcelona, Spain. [14]Memorial Sloan Kettering Cancer Center, New York, New York. [15]Abramson Cancer Center, University of Pennsylvania, Philadelphia, Pennsylvania. [16]Department of Medical Oncology, University Medical Center Utrecht, Utrecht University, Utrecht, the Netherlands. [17]University Hospitals Leuven and KU Leuven, Leuven, Belgium. [18]Novartis Pharma AG, Basel, Switzerland. [19]Novartis Pharmaceuticals Corporation, East Hanover, NJ. [20]Massachusetts General Hospital Cancer Center and Department of Medicine, Harvard Medical School, Boston, Massachusetts.

Running Title: Transcriptional Subtype and BRAF/MEK/EGFR Blockade in CRC

Corresponding Author (Full Name, Mailing Address, Phone and Fax, and Email):

Gary Middleton
Institute of Immunology and Immunotherapy (III)
College of Medical and Dental Sciences
Vincent Drive
University of Birmingham
Birmingham, B15 2TT
United Kingdom
Phone: 0121 415 8237
Fax: 0121 414 4486
Email: g.middleton@bham.ac.uk

Conflict of Interest Disclosure Statement:

GM reported research funding from Novartis. **YY** reported employment with Novartis. **CDC** reported employment and equity ownership with Novartis and employment for her spouse with Pfizer. **TA** has served in a consulting/advisory role and/or received honoraria for Amgen, Bristol-Myers Squibb, Chugai, Halliodx, MSD Oncology, Pierre Fabre, Roche/Ventana, Sanofi, Servier; has received travel, accommodations, and expenses from Roche/Genentech, MSD Oncology, and Bristol-Myers Squibb. **CEA** reported research funding from Bristol-Myers Squibb, Kura Oncology, Guardant Health, Merck, and Novartis; advisory board for Array Biopharma, Pionyr Immunotherapeutics. **JHMS** reported equity ownership of, honoraria from, and patents and royalties from Modra Pharmaceuticals. **JCBe** reported research funding to institution from Gilead, Genentech/Roche, Bristol-Myers Squibb, Five Prime, Lilly, Merck, MedImmune, Celgene, EMD Serono, Taiho, Macrogenics, GSK, Novartis, OncoMed, LEAP, TG Therapeutics, AstraZeneca, BI, Daiichi Sankyo, Bayer, Incyte, Apexigen, Koltan, SynDevRex, Forty Seven, AbbVie, Array, Onyx, Sanofi, Takeda, Eisai, Celldex, Agios, Cytomx, Nektar, ARMO, Boston Biomedical, Ipsen, Merrimack, Tarveda, Tyrogenex, Oncogenex, Marshall Edwards, Pieris, Mersana, Calithera, Blueprint, Evelo, FORMA, Merus, Jacobio, Effector, Novocare, Arrys, Tracon, Sierra, Innate, Arch Oncology, Prelude Oncology, Unum Therapeutics, Vyriad, Harpoon, ADC, Amgen, Pfizer, Millennium, Imclone, Acerta Pharma, Rgenix, Bellicum, Gossamer Bio, and Arcus Bio; consulting/advisory role to institution with Gilead, Genentech/Roche, Bristol-Myers Squibb, Five Prime, Lilly, Merck, MedImmune, Celgene, Taiho, Macrogenics, GlaxoSmithKline, Novartis, OncoMed, LEAP, TG Therapeutics, AstraZeneca, BI, Daiichi Sankyo, Bayer, Incyte, Apexigen, Array, Sanofi, ARMO, Ipsen, Merrimack, Oncogenex, FORMA, Arch Oncology, Prelude Therapeutics, Phoenix Bio, Cyteir, Molecular Partners, Innate, Torque, Tizona, Janssen, Tolero, TD2 (Translational Drug Development), Amgen, Seattle Genetics, Moderna Therapeutics, Tanabe Research Laboratories, Beigene, Continuum Clinical, and Agois; has received food/beverage/travel from Gilead, Genentech/Roche, Bristol-Myers Squibb, Lilly, Merck, MedImmune, Celgene, Taiho, Novartis, OncoMed, BI, ARMO, Ipsen, Oncogenex, and FORMA. **SS** reported advisory board with Amgen, Bayer, Bristol-Myers Squibb, Checkmate, Celgene, Clovis, Daichi-Sankyo, Incyte, Merck, Novartis, Roche/Genentech, and Seatlle Genetics. **JT** reported consultancy with Array Biopharma, AstraZeneca, Bayer, BeiGene, Boehringer Ingelheim, Chugai, Genentech, Inc., Genmab A/S, Halozyme, Imugene Limited, Inflection Biosciences Limited, Ipsen, Kura Oncology, Lilly, MSD, Menarini, Merck Serono, Merrimack, Merus, Molecular Partners, Novartis, Peptomyc, Pfizer, Pharmacyclics, ProteoDesign SL, Rafael Pharmaceuticals, F. Hoffmann-La Roche Ltd, Sanofi, SeaGen, Seattle Genetics, Servier, Symphogen, Taiho, VCN Biosciences, Biocartis, Foundation Medicine, HalioDX SAS and Roche Diagnostics. **RY** reported research funding from Array BioPharma, Genentech, GlaxoSmithKline, Novartis; consulting for Array BioPharma. **PJO** reported research support from Pfizer, Genentech, Bristol-Meyers Squibb, GlaxoSmithKline, Five

Prime, Forty Seven, BBI, Novartis, Celgene, Incyte, Lilly/Imclone, Array, H3 Biomedicine, and Taiho; consulting in the past 2 years with Genentech, Celgene, and Array; expert testimony with Bayer and Lilly. **EV** reported. **JMM** reported employment and equity ownership with Novartis. **JCBr** reported employment and stocks with Novartis. **FR** reported employment with Shattuck Labs and former employment with Novartis. **EG** reported employment and equity ownership with Novartis. **RC** reported consultancy with Amgen, Avidity Biosciences, Array, Astex, C4 Therapeutics, Elicio, FOG Pharma, Fount Therapeutics, Genentech, LOXO, N-of-One, Novartis, nRichDx, Revolution Medicines, Roche, Roivant, Shionogi, Spectrum, Taiho, Warp Drive Bio; equity ownership with Avidity Biosciences, C4 Therapeutics, Fount Therapeutics, nRichDx, Revolution Medicines; research funding from Asana, AstraZeneca; honoraria from Symphogen, Chugai; and advisory board payments from C4 Therapeutics, Fount Therapeutics, and nRichDx. **All authors** received support for third-party medical writing and editorial assistance provided by ArticulateScience LLC, funded by Novartis Pharmaceuticals Corporation.

Statement of Translational Relevance

There is increasing evidence to support a role for combined BRAF/MEK/EGFR inhibition in the treatment of *BRAF*-mutant colorectal cancer. The present study demonstrates the importance of considering the transcriptional context of mutations before applying targeted therapy, highlighting the identification of BM subtype as critical for optimal patient selection.

Abstract

Purpose: The influence of the transcriptional and immunologic context of mutations on therapeutic outcomes with targeted therapy in cancer has not been well defined. *BRAF* V600E–mutant (BM) colorectal cancer comprises two main transcriptional subtypes, BM1 and BM2. We sought to determine the impact of BM subtype, as well as distinct biological features of those subtypes, on response to BRAF/MEK/EGFR inhibition in patients with CRC.

Experimental Design: Paired fresh tumor biopsies were acquired at baseline and on day 15 of treatment from all consenting patients with BM CRC enrolled in a Phase II clinical trial of dabrafenib, trametinib, and panitumumab. For each sample, BM subtype, cell cycle, and immune gene signature expression were determined using RNA-sequencing (RNA-seq), and a Cox proportional hazards model was applied to determine association with progression-free survival (PFS).

Results: Confirmed response rates, median PFS, and overall survival (OS) were higher in BM1 subtype patients compared to BM2 subtype patients. Evaluation of immune contexture identified greater immune reactivity in BM1, while cell cycle signatures were more highly expressed in BM2. A multivariate model of PFS incorporating BM subtype plus immune and cell cycle signatures revealed that BM subtype encompasses the majority of the effect.

Conclusion: BM subtype is significantly associated with the outcome of combination dabrafenib, trametinib, and panitumumab therapy and may serve as a standalone predictive biomarker beyond mutational status. Our findings support a more nuanced approach to targeted therapeutic decisions that incorporates assessment of transcriptional context.

Introduction

The stratification of patients for targeted anticancer therapy is currently based on identification of the required genetic aberration with little, if any, consideration given to the impact of the biological context in which the mutation is found. The context dependency of canonical mutations across different cancer types is well recognized. For example, although patients with melanoma and lung cancer harboring the *BRAF* V600E mutation often respond well to dual BRAF and mitogen-activated protein kinase (MAPK) kinase (MEK) inhibition (1-4), this same approach usually fails to provide meaningful benefit to patients with colorectal cancer (CRC) whose cancers harbor the same mutation (5,6). However, it is now clear that canonical mutations in CRC can occur in very different transcriptional and immunobiological contexts. Whether these varying contexts influence therapeutic outcomes with targeted therapies stratified by genotype is currently unknown.

Four consensus molecular subtypes (CMS1-CMS4) based on gene expression patterns have been defined within CRC (7). Although *BRAF* mutations tend to be more prevalent in CMS1 (microsatellite instability [MSI]/immune) CRC, they can also be found in CMS3 (metabolic) and CMS4 (mesenchymal) CRC. Furthermore, two transcriptional subtypes of *BRAF* V600E-mutant (BM) CRC (BM1 and BM2) have been described, with the BM1 subtype associated with a poorer prognosis than the BM2 subtype (8). BM1 is characterized by KRAS/AKT pathway activation; epithelial–mesenchymal transition (EMT) that mediates invasion, metastasis, and chemotherapy resistance (9); and increased immune reactivity. In contrast, BM2 demonstrates deregulation of cell cycle checkpoints. Importantly, BM1 CRC cell lines appear to be more sensitive to BRAF and MEK inhibition, while BM2 lines are more sensitive to cyclin-dependent kinase 1 inhibition. As a further example of the variable context in which particular mutations are found, *KRAS* mutation—the most common canonical mutation in CRC—occurs across all 4 CMS subtypes and thus may occur in the context of both different transcriptional programs and in cancers with widely differing levels of immune reactivity (7,9). Therefore, inferring the likely biology and thus the therapeutic vulnerability of a given mutation in CRC is impossible without consideration of the transcriptional and immunologic context in which that mutation is found.

We recently reported the outcomes in patients with BM CRC treated with various combinations of the BRAF inhibitor dabrafenib (D), the MEK inhibitor trametinib (T), and the epidermal growth factor receptor (EGFR) inhibitor panitumumab (P) (10). Combination therapy is given with the goal of mitigating the MAPK pathway reactivation upon BRAF inhibition, which in CRC occurs as the result of an initial decrease in extracellular signal-regulated kinase (ERK) activation. This triggers enhanced EGFR/KRAS signaling, which drives BRAF/CRAF and CRAF/CRAF dimerization, thus reactivating MEK and ultimately resulting in suboptimal ERK inhibition (11,12). Although this EGFR-mediated RAS hyperactivation is certainly a key factor in limiting the efficacy of BRAF/MEK blockade, there must be additional factors contributing to this poor response in CRC, given that BRAF/MEK inhibitor

combinations have proven effective in lung cancer, which is also a characteristically EGFR-expressing malignancy.

Herein we explore the premise that other biological characteristics of BM CRC limit responsiveness to BRAF inhibitor-based combinatorial targeted therapy approaches. Given the distinct biology of the BM1 and BM2 transcriptional subtypes, we analyzed the impact of transcriptional context on outcomes in patients with BM CRC treated with combination D+T+P. Our findings demonstrate for the first time that the transcriptional context of a targeted mutation in a single cancer type does indeed significantly influence the response to therapy. Specifically, the BM1 subtype of CRC responds relatively favorably to BRAF/MEK/EGFR inhibition, while patients with the more common BM2 subtype appear to derive limited benefit from this approach. These data suggest that, to optimize outcomes with targeted therapies, a more nuanced approach to therapeutic decision making may be required that is informed by biology beyond the known targeted mutation. This supplemental stratification is critical to improving the risk-benefit equation for these often expensive and potentially toxic therapies. Such optimization is particularly relevant in situations where a limited proportion of patients derive meaningful benefit or where the mutation targeted does not appear to contribute to oncogene addiction in that cancer.

Materials and Methods

Patients/Samples

As described in Corcoran et al (10), paired fresh tumor biopsies were acquired prior to treatment (baseline) and on day 15 of treatment for all enrolled patients who gave consent. The appropriate ethics committee or institutional review board at each study center approved the study protocol. The study was conducted in accordance with Guidelines for Good Clinical Practice and the ethical principles described in the Declaration of Helsinki following all applicable local regulations. All patients provided written informed consent prior to enrollment. Most biopsies were flash-frozen samples; a small number were formalin-fixed paraffin-embedded tissue initially acquired for *BRAF* V600 mutation testing. All samples were shipped to a central laboratory for subsequent analysis and processed for RNA sequencing as described below.

RNA-Seq

RNA was extracted from fresh frozen and formalin-fixed paraffin-embedded tissue biopsies using Maxwell RNA extraction kits (Promega #AS1280). To enrich for mRNA, rRNA was depleted using RNase H digestion. The rRNA-depleted RNA was fragmented, converted to cDNA, and constructed into sequencing libraries with the TruSeq RNA Library Preparation Kit v2 (Illumina #RS-122-2001 and #RS-122-2002). The resulting libraries were sequenced with 100-bp paired-end reads to a target depth of 50 million total reads per sample on an Illumina HiSeq.

Next-Generation Sequencing Data Processing

Sequencing reads were aligned to the human reference genome (hg19) using STAR (13). HTSeq was used to quantify the number of reads aligned to each gene in the RefSeq transcriptome (14). Sequencing data were evaluated for quality, and low-complexity libraries with < 2 million estimated unique read pairs were excluded from downstream analysis. In total, 140 samples were compatible with downstream analysis, including 80 baseline samples and 60 on-treatment samples primarily collected after 2 weeks of therapy. Gene count data were normalized using the trimmed mean of M values method as implemented in edgeR (15). All downstream gene signature analyses were performed on the $\log_2$ of the normalized gene count data, after adding 0.1 to all gene counts to avoid taking the $\log_2$ of 0.

Subtype Classification

BM subtype classification was performed using the classifier described in Barras et al. (8) and the code made available by the authors of that study (http://bcf.isb-sib.ch/Projects/CRC_BRAFmut_subtypes.html). BM subtype classification was compared with the clusters obtained with hierarchical clustering based on the Ward method (16) using gene expression for the genes reported as differentially expressed between BM1 and BM2 (8) that overlapped our RNA-seq gene expression results (N = 467). CMS subtype classification was performed using the

classifier implemented in the CMSClassifer R package (Sage Bionetworks; https://github.com/Sage-Bionetworks/CMSclassifier) using the single sample predictor method.

Gene Signature Analysis

Immune gene expression signatures were derived by clustering tumor gene expression from The Cancer Genome Atlas into modules of highly correlated genes. Each module was then assigned by expert curation to a particular immune cell type where possible. The 20 signatures that could be assigned to a unique immune cell type were then evaluated in the gene expression data generated for the clinical samples. Expression of immune signatures was calculated as the mean of the $\log_2$ normalized expression of all genes in each gene signature. The specific genes that each immune signature is composed of are listed in **Supplementary Table S1**.

Statistics and Multivariate Modeling

The D+T+P population was used for the multivariate analysis, which contained two steps. The first step was to prescreen for those immune gene signatures that were significantly associated with PFS. A Cox proportional hazards model was applied to each of the 20 immune gene signatures, including both BM subtype and baseline expression of the immune gene signature as covariates. Any immune signatures that emerged as significantly associated with PFS were selected and used in the subsequent second step of the multivariate analysis. In this final step, a Cox proportional hazards model was developed that included BM subtype, the pre-identified immune gene signatures associated with PFS, and the G2M cell cycle signature. All survival analyses were done in R version 3.4.3 using the survival 2.41-3 package (R Foundation).

Data Sharing and Availability

Novartis is committed to sharing with qualified external researchers, access to patient-level data and supporting clinical documents from eligible studies. These requests are reviewed and approved by an independent review panel on the basis of scientific merit. All data provided is anonymised to respect the privacy of patients who have participated in the trial in line with applicable laws and regulations. This trial data availability is according to the criteria and process described on www.clinicalstudydatarequest.com.

Results

We recently reported the clinical outcomes and initial tissue/blood biomarker results for patients with advanced BM CRC treated with 3 different combination regimens targeting the BRAF/MEK/EGFR pathway (trial registration ID: NCT01750918). The confirmed response rate (RR) with the D+T+P triplet combination was 21% (n = 19 out of 91), with an unconfirmed RR of 32% and a median progression-free survival (PFS) of 4.2 months (10). Confirmed RRs with the D+P doublet and the T+P doublet were 10% and 0%, respectively. Given this modest activity, and the cost and toxicity associated with these regimens, we investigated whether there were other predictive biomarkers for outcome beyond *BRAF* V600E mutational status. Specifically, we explored the possibility that the cancers in those patients who derived benefit from the combination had an underlying biology distinct from that in patients who derived no obvious benefit.

We first asked whether the transcriptional context in which the *BRAF* V600E mutation was found influenced response to therapy. We applied the recently described BM1 and BM2 transcriptional signatures (8) to RNA expression data generated using fresh-tissue biopsies from patients treated in the study, obtained for pharmacodynamic analyses and other translational work. From the D+T+P cohort, RNA-sequencing (RNA-seq) gene expression data were successfully obtained from 34 paired patient biopsy samples (day 1 and day 15) and 16 separate baseline biopsy samples from day 1 only, yielding baseline samples from 50 patients. Although this represents a meaningful sample set, analyzable samples were not available from all study participants: some pre-therapy samples failed during processing, while other patients either refused biopsy after registration or were found to have lesions unsuitable for biopsy.

Forty-six of 50 baseline biopsies (92%) from D+T+P–treated patients were from metastatic sites: 26 hepatic, 9 nodal, 10 peritoneal/mesenteric/omental/intra-abdominal, and 1 from the chest wall. Baseline biopsies were also available from 30 total patients in the D+P and T+P cohorts. The distribution of biopsy sites from these cohorts was similar, with 26 of 30 (86%) taken from metastatic sites: 18 hepatic, 6 nodal, 1 peritoneal/mesenteric/omental/intra-abdominal, and 1 from the lung. Baseline characteristics—including median age, gender, Eastern Cooperative Oncology Group performance status, number of prior lines of therapy, prior anti-EGFR therapy (<20% for both subtypes), and primary tumor location—were similar between BM1 and BM2 patients (**Supplementary Table S2**). Thus, this biorepository represents a meaningful number of fresh, largely metastatic biopsy samples from patients with BM CRC.

We performed hierarchical clustering based on gene expression of 467 genes in our RNA-seq data set that overlapped with published reports of genes that are differentially expressed between BM1 and BM2 (8). The hierarchical clustering method closely reproduced the subtypes assigned by the published classifier (88% concordance between subtype assigned by hierarchical clustering based on expression of 467 genes in our RNA-seq library and subtype assigned by the

published classifier; **Fig. 1A**). BM1 and BM2 subtypes were distributed across all tissue sites, both primary and metastatic, sampled in this analysis. The proportion of BM1 tumors across all samples was 32%, consistent with the frequency seen in samples from resected patients (8). For 64 patients across all 3 combination therapies, we had information regarding both baseline BM subtype and MSI status; there was no difference observed in MSI-positive status between the two BM subtypes (BM1, 13.3% and BM2, 14.3% [Fisher $P > .99$]). However, there were clear differences in the distribution of CMS subtypes between the two BM subtypes. The majority of BM1 samples were CMS4, whereas there was a more even distribution of CMS subtypes across the BM2 samples that were classified (**Fig. 1B**).

Figure 2 shows the waterfall plot of best confirmed responses according to Response Evaluation Criteria in Solid Tumors (RECIST) in patients treated with the D+T+P combination, color-coded by BM subtype. The confirmed RR in BM1 patients was 38% compared with 7% in BM2 patients (Fisher *P* [two-tailed] = .01). A similar trend was seen for unconfirmed RR (BM1, 44% and BM2, 26% [$P = .32$]); however, this trend did not reach statistical significance. The discrepancy between the confirmed and unconfirmed RR in BM2 was due to the very short duration of response in BM2 (2.8 months compared with 7.6 months in BM1), leading to a lack of confirmation of response on the subsequent scan. BM subtype was also associated with PFS and overall survival (OS). The median PFS with D+T+P was 7.4 months in BM1 and 3 months in BM2 (HR, 4.33; log-rank $P = .0012$) (**Fig. 3A**). The median OS with D+T+P was 19.8 months in BM1 and 6.3 months in BM2 (HR, 3.37; log-rank $P = .012$) (**Fig. 3B**). Thus, despite the poorer outcomes for patients with resected BM1 CRC compared to those with the BM2 subtype, BM1 patients exhibit a higher response rate and longer survival with D+T+P treatment compared to BM2 patients (8).

The poor response to D+T+P in patients with the BM2 subtype was not due to a lack of downstream pathway suppression in this subtype. There were significant reductions from baseline in both phosphorylated ERK (pERK) and phosphorylated S6 (pS6) expression, as measured immunohistochemically, in the matched on-treatment biopsies taken from BM2 patients treated with D+T+P (**Supplementary Fig. S1**). In addition, significant suppression of MAPK activity, as measured by MAPK pathway activity score (MPAS) gene signature expression (17), was also observed in the on-treatment samples taken from both BM1 and BM2 patients treated with D+T+P (**Supplementary Fig. S2**). Minimal or lack of MAPK suppression (log2FC > -0.25) was observed in a total of seven patients with paired baseline and on-treatment data: 4 out of 11 BM1 patients and 3 out of 23 BM2 patients. There was no significant association of BM subtype with this minimal or lack of MAPK suppression (Fisher $P = .18$).

To explore alternative possible reasons for the different outcomes observed in BM1 and BM2 patients, we first examined the differential baseline expression of the proapoptotic protein BIM between BM1 and BM2 subtypes. BIM levels are an

important determinant of the response of BM cells to MEK inhibition (18), and BIM was previously shown to be overexpressed in the BM1 subtype in primary cancer samples (8). However, we found no differences in BIM expression between BM1 and BM2 in our cohort of largely metastatic samples (**Supplementary Fig. S3A**). Alternatively, we hypothesized that greater dependency on pathway activation might underlie responsiveness in BM1 cancers, as enrichment of KRAS signaling signatures in BM1 has been previously demonstrated (8). The hallmark KRAS signature 5953, previously shown to be upregulated in BM1 relative to BM2, includes the *DUSP6*, *SPRY2*, *ETV4,* and *ETV5* genes, all of which predict sensitivity to MEK inhibition (19,20). We thus applied the parsimonious MPAS gene signature—which has been previously used in CRC (17) and contains the *CCND1*, *DUSP4*, *DUSP6*, *ETV4*, *ETV5*, *NT5E*, *SPRY2,* and *SPRY4* genes—to our sample set but found no difference in baseline expression between BM1 and BM2 and no association with clinical outcome regardless of BM subtype (**Supplementary Fig. S3B**). In contrast, the E2F and G2M cell cycle signatures previously identified as enriched in the BM2 subtype (8) were confirmed to be highly enriched at baseline in BM2 in our cohort, but change in cell cycle signature expression with D+T+P treatment was not significantly associated with clinical outcome (**Supplementary Fig. S4**).

Given that previous studies have shown that the efficacy of BRAF inhibitors is dependent on an intact immune system (21,22), we also analyzed the immune contexture of our sample set by evaluating the expression of a set of 20 immune gene signatures derived from modules of highly correlated genes, derived from gene expression data from The Cancer Genome Atlas and assigned by expert annotation to particular immune cell types (see **Methods** as well as **Supplementary Table S1** for the composition of the immune metagenes analyzed), 12 of which were more highly expressed in either BM1 or BM2. Overall, BM1 samples in our data set had significantly higher levels of immune infiltration, with 10 of the 12 differentially expressed immune metagenes exhibiting greater baseline expression in the samples taken from D+T+P–treated BM1 patients than in the samples from BM2 patients. Baseline expression of the T-cell (P = .008), cytotoxic cell (P = .033), Langerhans dendritic cell (DC; P = .0062), plasmacytoid DC (pDC)–like (P = .037), phagocytic C-type lectin domain containing 9A (CLEC9A; P = .003), macrophage (P = .02), M2 (P = .0019), fibroblast (P = 8.2e-06), mast cell (P = .0002), and regulatory T-cell (Treg; P = .0062) signatures was significantly greater in BM1 than in BM2 (**Fig. 4**). Only two immune metagenes, the polymorphonuclear neutrophil (PMN) 1 (P = .039) and neutrophil chemokine (P = .0017) signatures, exhibited the opposite pattern, with significantly higher expression in BM2 samples.

Of the 20 immune gene signatures investigated, three were also significantly associated with confirmed response, and this was true regardless of BM subtype (P < .05): the T-cell, memory B-cell, and phagocytic CLEC9A signatures; an association of the Treg signature with response was also observed (P = .078) (**Fig. 5**). Of note, these four immune signatures do not have any gene overlap with the BM1 or BM2

signatures, while the phagocytic CLEC9A signature had the greatest correlation with BM subtype of the four (**Table 1**). To assess whether these immune gene signatures associated with response were modulated on-treatment, we analyzed their expression in the biopsies taken from those patients (n = 34) with paired baseline and on-treatment samples. We observed significant increases in expression of the T-cell (*P* = .018) and phagocytic CLEC9A (*P* = .0013) signatures, and a borderline significant increase in the memory B-cell signature (*P* = .057), on-treatment; however, there was no significant difference in Treg signature expression from baseline (*P* = .59; **Supplementary Figure S5**). Moreover, we observed that, among the 20 immune gene signatures we investigated, some that were not significantly associated with response were nevertheless significantly upregulated in the on-treatment samples; thus, neither changes in immune gene signature expression on-treatment, nor the magnitude of such changes, were associated with response (**Supplementary Table S3**).

Given the differential expression of key immune and cell cycle gene signatures among BM subtypes, we questioned whether any of these gene signatures might contribute independently to treatment outcomes or if BM subtype alone encapsulates this effect. To that end, we performed a multivariate analysis of factors that may impact PFS with D+T+P treatment. First, we applied a Cox proportional hazards model to each of the 20 immune gene signatures to prescreen for those significantly associated (*P* < .05) with both PFS and BM subtype; association values for all of the immune gene signatures with PFS are listed in **Table 1**. This screening identified 8 immune gene signatures, all of which were positively associated with PFS, for which this association reached significance: T cell (*P* = .014), cytotoxic cell (*P* = .015), macrophage (*P* = .026), IFN-γ (*P* = .029), B-cell (*P* = .007), memory B-cell (*P* = .001), pDC-like (*P* = .02), and Treg (*P* = .015). We next applied a multivariate Cox proportional hazards model that included BM subtype as well as baseline expression of gene signatures that are associated with each BM subtype: the G2M cell cycle signature (for BM2) and the 8 immune metagenes that were identified to be associated with PFS (for BM1). Of the factors included in the multivariate analysis, only BM subtype emerged as associated with PFS (**Table 2**; HR, 5.12; *P* = .017). This demonstrates that BM subtype has a significant independent effect on PFS and encapsulates the majority of the outcome of differential immune and cell cycle gene signature expression. Thus, BM subtype appears to be an independent predictive biomarker, beyond mutational status, of outcome with combinatorial BRAF/MEK/EGFR-based therapy that should be considered during therapeutic selection for patients with BM CRC.

Discussion

We have demonstrated that patients with BM1-subtype CRC have a significantly better RR, median duration of response, and median PFS and OS than patients with BM2-subtype disease when treated with the D+T+P combination. The BM1 RR of 38%—with median response duration, PFS, and OS of 7.6, 7.4, and 19.8 months, respectively—is meaningful and of therapeutic value. However, the median PFS and OS in BM2 patients treated with D+T+P were only 3 and 6 months, respectively, with < 10% of patients having a confirmed response to therapy. The median PFS we observed with BM2 patients is similar to the median post-progression survival after failure of first-line chemotherapy observed in patients with metastatic BM CRC (23). Thus, given the toxicity and expense of combinatorial regimens, these observations suggest that consideration should be given to restricting the use of D+T+P, as well as analogous combinations targeting the BRAF/MEK/EGFR pathway, to BM1 patients.

The results of the randomized phase III BEACON trial (trial registration ID: NCT02928224) have recently been published, in which the triplet BRAF/MEK/EGFR inhibitor combination of encorafenib, binimetinib, and cetuximab significantly improved overall survival (OS) compared with the control arm of cetuximab plus investigator's choice chemotherapy in patients with BM CRC. The outcomes measures for the triplet regimen used in BEACON were similar to those observed with D+T+P: median OS was 9 months, median PFS was 4.3 months, and the confirmed objective RR was 26% (24). Thus, with both D+T+P and the BEACON triplet combination, only approximately 25% of patients with BM CRC had an objective response to therapy, and only 50% of those patients were progression free beyond 4 to 5 months. Moreover, we found that D+T+P treatment was associated with a median OS of 19.8 months in BM1 CRC patients, a substantial increase over the 9-month median OS observed in the broader BEACON patient population (10). It is important to note that BM1 patients tend to have a worse outcome than BM2 patients (8), and so these outcome data with targeted therapy are particularly noteworthy. These results indicate that BM subtype could represent a key biomarker to aid in the appropriate selection of those patients with BM CRC who are more likely to benefit from combinatorial BRAF/MEK/EGFR inhibition, and suggest that these results should be validated in ongoing studies of the encorafenib, binimetinib, and cetuximab combination. To our knowledge, the present report is the first in which the transcriptional context of a tumor bearing a canonical mutation has been shown to impact responses to therapy targeting that mutation.

Preclinical studies have demonstrated that immune reactivity is critical to the efficacy of *BRAF* V600 inhibition in BM cancers. Depletion of $CD8^+$ T cells abrogated the efficacy of the BRAF inhibitor vemurafenib in a vemurafenib-sensitive transplantable BRAF/PTEN mouse model but had no effect on tumor growth in untreated control mice (25). $CD4^+$ T cells have also been shown to be important for the efficacy of the vemurafenib precursor compound PLX4720 (22). The neutralization of IFN-γ and abrogation of CD40/CD40-ligand signaling reduced the efficacy of BRAF inhibition,

and IFN-γ and vemurafenib have synergistic effects in limiting the growth of both murine and human BM cancer cells (21,22). Finally, $CD8^+$ T-cell density has been shown to independently impact PFS in patients with BM melanoma treated with either BRAF inhibitor monotherapy or BRAF/MEK inhibitor combination therapy (26).

Our findings demonstrate that BM1-subtype CRC is immunologically enriched relative to the BM2 subtype, while responders regardless of transcriptional subtype had higher expression of the T-cell, memory B-cell, Treg, and phagocytic CLEC9A signatures compared with nonresponders. Although the positive impact of T-cell density on CRC outcomes is well described, T cells are tightly associated with B cells in CRC, and B-cell density is a positive prognostic marker in CRC (27,28). B cells positively modulate T-cell responses through antigen presentation, provision of costimulation, and cytokine release (29). Alongside B cells, $BDCA3^+$ myeloid DCs appear to be the main cross-presenting cell type and the main source of cross-presenting antigen from necrotic cancer cells (30). CLEC9A is selectively expressed by this DC subset in humans and can cross-present to both $CD8^+$ and $CD4^+$ T cells (31). Although the association between Tregs and CRC outcomes appears counterintuitive, it is well known that in CRC, $FoxP3^+$ Tregs infiltrate both the epithelium and stroma and are significantly positively associated with OS, in contrast to the poor outcomes seen with high Treg infiltration in most other cancers (32). This finding has been attributed to the unique microenvironment of primary CRC, where Tregs may be important in limiting the inflammatory response initiated by bacterial translocation and the deleterious effects of T_H17 cells (33). While the majority of differentially expressed immune gene signatures were enriched in BM1, the chemokine neutrophil and PMN 1 signatures are notable exceptions that were instead enriched in BM2. In some studies, neutrophils play a role in creating an unfavorable tumor microenvironment, and a high neutrophil-to-lymphocyte ratio is predictive of poor response in CRC (34,35). In a multivariate model that included BM subtype as well as key immune and cell cycle gene signatures, the only factor that independently predicted improved PFS with combinatorial BRAF/MEK/EGFR blockade was BM subtype. Thus, BM subtype captures much of the diverse biology, including the immunobiology, of BM CRC, which might in part explain the differences in therapeutic outcomes observed between BM1 and BM2 patients.

The majority of the BM1 cancer biopsy samples taken from metastatic sites of patients with BM CRC were of the CMS4 subtype. CMS4 is the mesenchymal subtype characterized by upregulation of EMT genes and activation of TGF-β signaling (7). In early-stage resected BM CRC, all CMS4 tumors were found to belong to the BM1 subtype (8); our work demonstrates that metastatic BM1 cancers are also largely of the EMT-enriched CMS4 subtype. *BRAF* V600E activation is characteristic of the sessile serrated adenoma (SSA) pathway. SSAs are molecularly and histologically distinct from the main precursor lesion of CRC, the tubular adenoma. The strength of TGF-β signaling was found to be of critical importance in determining whether SSAs adopt a CMS1 or CMS4 transcriptional program. Tubular

adenomas could be clearly distinguished from SSAs using a TGF-β response signature because of higher expression in the latter and, as expected, the signature could segregate CMS4 from CMS1-CMS3 cancers. Interestingly, the response signature clustered the SSAs into two groups: those with the highest expression of TGF-β were of the CMS4 subtype, and those with the lowest were CMS1. These data strongly suggest that the differentiation of SSAs into CMS1 or CMS4 cancer is dependent on the strength of TGF-β signaling. Consistently, TGF-β–related genes were more highly expressed in the SSAs classified as CMS4 than in SSAs classified as CMS1. Unlike *BRAF* wild-type tubular adenomas, organoid cultures carrying *BRAF* V600E did not undergo apoptosis when treated with TGF-β but instead had a strong induction of EMT in the majority of cells, suggestive of SSA origins (36). Thus, metastatic BM1 cancers appear to originate from SSA lesions that progress to carcinoma under the influence of strong TGF-β signaling which, in turn, activates EMT and angiogenesis. Finally, some of the previously identified molecular differences between BM1 and BM2 were not replicated in the current study, including subtype differences in signatures of MAPK pathway activation (8). However, > 90% of samples analyzed in the current study were from metastatic sites rather than primary tumors, and the impact of BM subtype on the degree of MAPK pathway activation is unknown.

In summary, we have shown that the BM1 subtype of metastatic CRC represents the majority of metastatic BM CMS4 cancers, a known aggressive molecular phenotype (7). However, these cancers demonstrate useful clinical sensitivity to BRAF/MEK/EGFR inhibition with D+T+P. In contrast, BM2 cancers appear to be relatively insensitive to D+T+P triplet blockade, suggesting these patients may be better served by other treatment regimens. We acknowledge that the sample size of the current study is relatively small, and thus these observations require further validation. However, they suggest that BM1 subtype may be an important predictive marker for the efficacy of BRAF pathway–targeted therapy in BM CRC, a particularly important finding, given the cost and potential toxicity of these combinations. This is the first demonstration, to our knowledge, that the transcriptional contexture of a canonical mutation impacts outcome with targeted therapy directed against that mutation. These results suggest that ongoing trials of combination targeted therapy for CRC should stratify patients by BM subtype and that such trials in patients selected for BM1 subtype are warranted. Moreover, assessing the association between BM subtype and outcomes with other therapeutic regimens in CRC will help to elucidate whether this is a specific interaction between BM1 and BRAF pathway-targeted therapy, or if there is a more generalizable impact of BM subtype on outcomes to different treatment modalities in CRC.

Acknowledgements

This study was supported by GlaxoSmithKline and Novartis. As of March 2, 2015, dabrafenib and trametinib are assets of Novartis AG. The authors would like to acknowledge the investigators of this trial for providing all the biopsies that were so critical to this work. The authors would also like to thank Ilona Tala for assistance with biosample management and Rebecca Leary for her efforts in directing the lab work associated with this study as well as helpful scientific discussion. Medical writing assistance was provided by Amy Ghiretti, PhD (ArticulateScience LLC), funded by Novartis Pharmaceuticals Corporation.

References

1. Hauschild A, Grob J-J, Demidov LV, Jouary T, Gutzmer R, Millward M*, et al.* Dabrafenib in BRAF-mutated metastatic melanoma: a multicentre, open-label, phase 3 randomised controlled trial. The Lancet **2012**;380(9839):358-65.
2. Long GV, Stroyakovskiy D, Gogas H, Levchenko E, de Braud F, Larkin J*, et al.* Dabrafenib and trametinib versus dabrafenib and placebo for Val600 BRAF-mutant melanoma: a multicentre, double-blind, phase 3 randomised controlled trial. Lancet **2015**;386(9992):444-51.
3. Planchard D, Kim TM, Mazieres J, Quoix E, Riely G, Barlesi F*, et al.* Dabrafenib in patients with BRAFV600E-positive advanced non-small-cell lung cancer: a single-arm, multicentre, open-label, phase 2 trial. The Lancet Oncology **2016**;17(5):642-50.
4. Planchard D, Smit EF, Groen HJM, Mazieres J, Besse B, Helland Å*, et al.* Dabrafenib plus trametinib in patients with previously untreated BRAFV600E-mutant metastatic non-small-cell lung cancer: an open-label, phase 2 trial. The Lancet Oncology **2017**;18(10):1307-16.
5. Corcoran RB, Atreya CE, Falchook GS, Kwak EL, Ryan DP, Bendell JC*, et al.* Combined BRAF and MEK inhibition With dabrafenib and trametinib in BRAF V600-mutant colorectal cancer. J Clin Oncol **2015**;33(34):4023-31.
6. Kopetz S, Desai J, Chan E, Hecht JR, O'Dwyer PJ, Maru D*, et al.* Phase II pilot study of vemurafenib in patients With metastatic BRAF-mutated colorectal cancer. J Clin Oncol **2015**;33(34):4032-8.
7. Guinney J, Dienstmann R, Wang X, de Reynies A, Schlicker A, Soneson C*, et al.* The consensus molecular subtypes of colorectal cancer. Nat Med **2015**;21(11):1350-6.
8. Barras D, Missiaglia E, Wirapati P, Sieber OM, Jorissen RN, Love C*, et al.* BRAF V600E mutant colorectal cancer subtypes based on gene expression. Clin Cancer Res **2017**;23(1):104-15.
9. Lal N, White BS, Goussous G, Pickles O, Mason MJ, Beggs AD*, et al.* KRAS mutation and consensus molecular subtypes 2 and 3 are independently associated with reduced immune infiltration and reactivity in colorectal cancer. Clin Cancer Res **2018**;24(1):224-33.
10. Corcoran RB, Andre T, Atreya CE, Schellens JHM, Yoshino T, Bendell JC*, et al.* Combined BRAF, EGFR, and MEK inhibition in patients with BRAF(V600E)-mutant colorectal cancer. Cancer Discov **2018**;8(4):428-43.
11. Corcoran RB, Ebi H, Turke AB, Coffee EM, Nishino M, Cogdill AP*, et al.* EGFR-mediated re-activation of MAPK signaling contributes to insensitivity of BRAF mutant colorectal cancers to RAF inhibition with vemurafenib. Cancer Discov **2012**;2(3):227-35.
12. Prahallad A, Sun C, Huang S, Di Nicolantonio F, Salazar R, Zecchin D*, et al.* Unresponsiveness of colon cancer to BRAF(V600E) inhibition through feedback activation of EGFR. Nature **2012**;483(7387):100-3.
13. Dobin A, Davis CA, Schlesinger F, Drenkow J, Zaleski C, Jha S*, et al.* STAR: ultrafast universal RNA-seq aligner. Bioinformatics **2013**;29(1):15-21.
14. Anders S, Pyl PT, Huber W. HTSeq--a Python framework to work with high-throughput sequencing data. Bioinformatics **2015**;31(2):166-9.
15. Robinson MD, McCarthy DJ, Smyth GK. edgeR: a Bioconductor package for differential expression analysis of digital gene expression data. Bioinformatics **2010**;26(1):139-40.

16. Murtagh F, Legendre P. Ward's hierarchical agglomerative clustering method: which algorithms implement Ward's criterion? Journal of Classification **2014**;31(3):274-95.
17. Wagle MC, Kirouac D, Klijn C, Liu B, Mahajan S, Junttila M*, et al.* A transcriptional MAPK Pathway Activity Score (MPAS) is a clinically relevant biomarker in multiple cancer types. NPJ Precis Oncol **2018**;2(1):7.
18. Cragg MS, Jansen ES, Cook M, Harris C, Strasser A, Scott CL. Treatment of B-RAF mutant human tumor cells with a MEK inhibitor requires Bim and is enhanced by a BH3 mimetic. J Clin Invest **2008**;118(11):3651-9.
19. Dry JR, Pavey S, Pratilas CA, Harbron C, Runswick S, Hodgson D*, et al.* Transcriptional pathway signatures predict MEK addiction and response to selumetinib (AZD6244). Cancer Res **2010**;70(6):2264-73.
20. Pratilas CA, Taylor BS, Ye Q, Viale A, Sander C, Solit DB*, et al.* (V600E)BRAF is associated with disabled feedback inhibition of RAF-MEK signaling and elevated transcriptional output of the pathway. Proc Natl Acad Sci U S A **2009**;106(11):4519-24.
21. Acquavella N, Clever D, Yu Z, Roelke-Parker M, Palmer DC, Xi L*, et al.* Type I cytokines synergize with oncogene inhibition to induce tumor growth arrest. Cancer Immunol Res **2015**;3(1):37-47.
22. Ho PC, Meeth KM, Tsui YC, Srivastava B, Bosenberg MW, Kaech SM. Immune-based antitumor effects of BRAF inhibitors rely on signaling by CD40L and IFNgamma. Cancer Res **2014**;74(12):3205-17.
23. Seligmann JF, Fisher D, Smith CG, Richman SD, Elliott F, Brown S*, et al.* Investigating the poor outcomes of BRAF-mutant advanced colorectal cancer: analysis from 2530 patients in randomised clinical trials. Ann Oncol **2017**;28(3):562-8.
24. Kopetz S, Grothey A, Yaeger R, Van Cutsem E, Desai J, Yoshino T*, et al.* Encorafenib, binimetinib, and cetuximab in BRAF V600E-mutated colorectal cancer. N Engl J Med **2019**;381(17):1632-43.
25. Steinberg SM, Zhang P, Malik BT, Boni A, Shabaneh TB, Byrne KT*, et al.* BRAF inhibition alleviates immune suppression in murine autochthonous melanoma. Cancer Immunol Res **2014**;2(11):1044-50.
26. Massi D, Romano E, Rulli E, Merelli B, Nassini R, De Logu F*, et al.* Baseline beta-catenin, programmed death-ligand 1 expression and tumour-infiltrating lymphocytes predict response and poor prognosis in BRAF inhibitor-treated melanoma patients. Eur J Cancer **2017**;78:70-81.
27. Bindea G, Mlecnik B, Tosolini M, Kirilovsky A, Waldner M, Obenauf AC*, et al.* Spatiotemporal dynamics of intratumoral immune cells reveal the immune landscape in human cancer. Immunity **2013**;39(4):782-95.
28. Mlecnik B, Van den Eynde M, Bindea G, Church SE, Vasaturo A, Fredriksen T*, et al.* Comprehensive intrametastatic immune quantification and major impact of immunoscore on survival. J Natl Cancer Inst **2018**;110(1).
29. Lund FE, Randall TD. Effector and regulatory B cells: modulators of CD4+ T cell immunity. Nat Rev Immunol **2010**;10(4):236-47.
30. Jongbloed SL, Kassianos AJ, McDonald KJ, Clark GJ, Ju X, Angel CE*, et al.* Human CD141+ (BDCA-3)+ dendritic cells (DCs) represent a unique myeloid DC subset that cross-presents necrotic cell antigens. J Exp Med **2010**;207(6):1247-60.
31. Schreibelt G, Klinkenberg LJ, Cruz LJ, Tacken PJ, Tel J, Kreutz M*, et al.* The C-type lectin receptor CLEC9A mediates antigen uptake and (cross-

)presentation by human blood BDCA3+ myeloid dendritic cells. Blood **2012**;119(10):2284-92.
32. Hu G, Li Z, Wang S. Tumor-infiltrating FoxP3(+) Tregs predict favorable outcome in colorectal cancer patients: A meta-analysis. Oncotarget **2017**;8(43):75361-71.
33. Ladoire S, Martin F, Ghiringhelli F. Prognostic role of FOXP3+ regulatory T cells infiltrating human carcinomas: the paradox of colorectal cancer. Cancer Immunol Immunother **2011**;60(7):909-18.
34. Haram A, Boland MR, Kelly ME, Bolger JC, Waldron RM, Kerin MJ. The prognostic value of neutrophil-to-lymphocyte ratio in colorectal cancer: A systematic review. J Surg Oncol **2017**;115(4):470-9.
35. Mizuno R, Kawada K, Itatani Y, Ogawa R, Kiyasu Y, Sakai Y. The role of tumor-associated neutrophils in colorectal cancer. Int J Mol Sci **2019**;20(3).
36. Fessler E, Drost J, van Hooff SR, Linnekamp JF, Wang X, Jansen M*, et al.* TGFbeta signaling directs serrated adenomas to the mesenchymal colorectal cancer subtype. EMBO Mol Med **2016**;8(7):745-60.

Table 1. Correlation of immune signature genes and BM signature genes

Signature	Genes in immune signature, n	Genes also in BM signature, n	Fraction of overlap	Correlation to BM1 genes	BM1 correlation *P* value	Correlation to BM2 genes	BM2 correlation *P* value	Association with PFS[a]
B-cell	8	0	0.00	0.42	2.08e-07	−0.30	2.92e-04	**0.49**
B-cell - memory	7	0	0.00	0.31	1.49e-04	−0.31	1.89e-04	**0.58**
Chemokine - myeloid	6	0	0.00	0.48	1.12e-09	−0.01	0.865397	0.53
Chemokine - neutrophil	6	0	0.00	−0.26	0.001523	0.55	1.35e-12	1.08
Cytotoxic cell	6	0	0.00	0.51	7.47e-11	−0.39	1.61e-06	**0.53**
Fibroblast	43	16	0.37	0.84	2.22e-39	−0.21	0.012268	1.57
IFN-γ	5	0	0.00	0.42	2.18e-07	−0.02	0.807672	**0.59**
Langerhans DC	10	0	0.00	0.56	4.55e-13	−0.38	3.49e-06	0.65
M2	9	2	0.22	0.79	3.53e-32	−0.49	5.39e-10	0.86
Macrophage	26	6	0.23	0.70	5.93e-22	−0.36	1.33e-05	**0.47**
Mast cell	12	0	0.00	0.66	3.46e-19	−0.25	0.003163	0.68
Osteoclast-like	6	0	0.00	0.35	1.63e-05	−0.02	0.824376	0.65
pDC-like	5	2	0.40	0.55	1.18e-12	−0.36	1.01e-05	**0.38**
Phagocytic CLEC9A	5	0	0.00	0.69	2.04e-21	−0.42	1.96e-07	0.57
PMN 1	5	0	0.00	0.00	0.988354	−0.09	0.29266	0.86
PMN 2	6	0	0.00	0.30	2.34e-04	−0.20	0.017794	0.71
PMN 3	6	0	0.00	0.12	0.147848	0.16	0.050639	0.69
T-cell	14	0	0.00	0.55	9.39e-13	−0.38	2.23e-06	**0.52**
Treg	10	0	0.00	0.50	2.51e-10	−0.16	0.052682	**0.41**
Type I IFN	14	0	0.00	0.22	0.007429	−0.05	0.57175	0.49

[a] An association of < 1 indicates that increased baseline expression of the immune gene signature is associated with longer PFS; an association of > 1 indicates that increased baseline expression of the immune gene signature is associated with shorter PFS. Significant associations ($P < .05$) are indicated in bold; all other association values are not significant and may be considered equivalent to 1 (no association with PFS).

Table 2. Multivariate analysis of the association between gene signature expression and PFS with D+T+P

Signature	Hazard Ratio (95% CI)	*P* Value
BM subtype	**5.12 (1.34-19.56)**	**0.017**
B-cell	0.76 (0.42-1.38)	0.367
B-cell - memory	1.49 (0.99-2.22)	0.055
Cytotoxic cell	0.7 (0.38-1.28)	0.248
IFN-γ	0.78 (0.5-1.22)	0.271
Macrophage	2.37 (0.89-6.28)	0.084
pDC-like	0.82 (0.32-2.05)	0.667
T-cell	0.84 (0.43-1.61)	0.593
Treg	1.1 (0.48-2.53)	0.82
G2M	1.89 (0.78-4.58)	0.158

The model incorporates the gene signature for BM subtype, 8 key immune gene signatures, and the G2M cell cycle gene signature. Note that the E2F and G2M cell cycle signatures are highly correlated (0.99); thus, only one (G2M) was included in the multivariate model.

Figure Legends

Figure 1. Characterization of the transcriptional and molecular subtypes of biopsy samples from patients with CRC. A, Determination of BM subtype via hierarchical clustering based on 467 published genes that are differentially expressed between BM1 and BM2 in baseline (N = 80) and on-treatment (N = 60) biopsies from patients treated with D+T+P, D+P, or D+T. Heat map shows the scaled-by-gene $\log_2$ counts per million gene expression data, with lower expression represented in blue and higher expression represented in red. BM subtype, as determined by published classifier and biopsy timepoint, is represented as horizontal bars above the heat map. Samples are ordered by hierarchical clustering based on Ward's D. **B,** Distribution of CMS subtypes across the two BM subtypes in baseline biopsy samples (n = 22 BM1; n = 60 BM2) from patients treated with D+T+P, D+P, or D+T. CMS subtype was determined using the published classifier [https://github.com/Sage-Bionetworks/CMSclassifier].

Figure 2. Increased rate of response to D+T+P in patients with BM1-subtype CRC. Waterfall plot showing maximum change in tumor size from baseline, colored by confirmed best response by RECIST in D+T+P–treated patients with baseline RNA-seq data (n = 47). BM subtype at baseline is represented by filled circles below the waterfall: BM1 (dark) and BM2 (light). Partial responses were observed in 6 of 16 BM1 patients and 2 of 31 BM2 patients.

Figure 3. BM1 subtype is associated with increased PFS and OS with combination BRAF/MEK/EGFR inhibition. A, PFS in BM1 (n = 16) and BM2 (n = 34) patients treated with D+T+P. **B,** OS in BM1 (n = 16) and BM2 (n = 34) patients treated D+T+P. *P* values represent BM1 vs BM2 by log-rank test.

Figure 4. Immune contexture of BM subtypes reveals increased immune infiltration in BM1-subtype CRC. Box plots show baseline expression of immune gene signatures in biopsy samples derived from BM1 (n = 16) vs BM2 (n = 34) patients treated with D+T+P. Of 20 immune metagenes tested, 12 were differentially expressed in BM1 vs BM2, including 10 more highly expressed in BM1. *P* values represent significance based on a nonparametric Wilcoxon rank sum test.

Figure 5. Key immune metagenes are associated with confirmed response to BRAF/MEK/EGFR inhibitor combination therapy regardless of BM subtype. Box plots show T-cell, memory B-cell, Treg, and phagocytic CLEC9A signature expression levels in confirmed responders (patients with partial response via RECIST) and nonresponders (patients with stable or progressive disease via RECIST) across BM subtypes. *P* values were derived using a two-tailed *t* test.

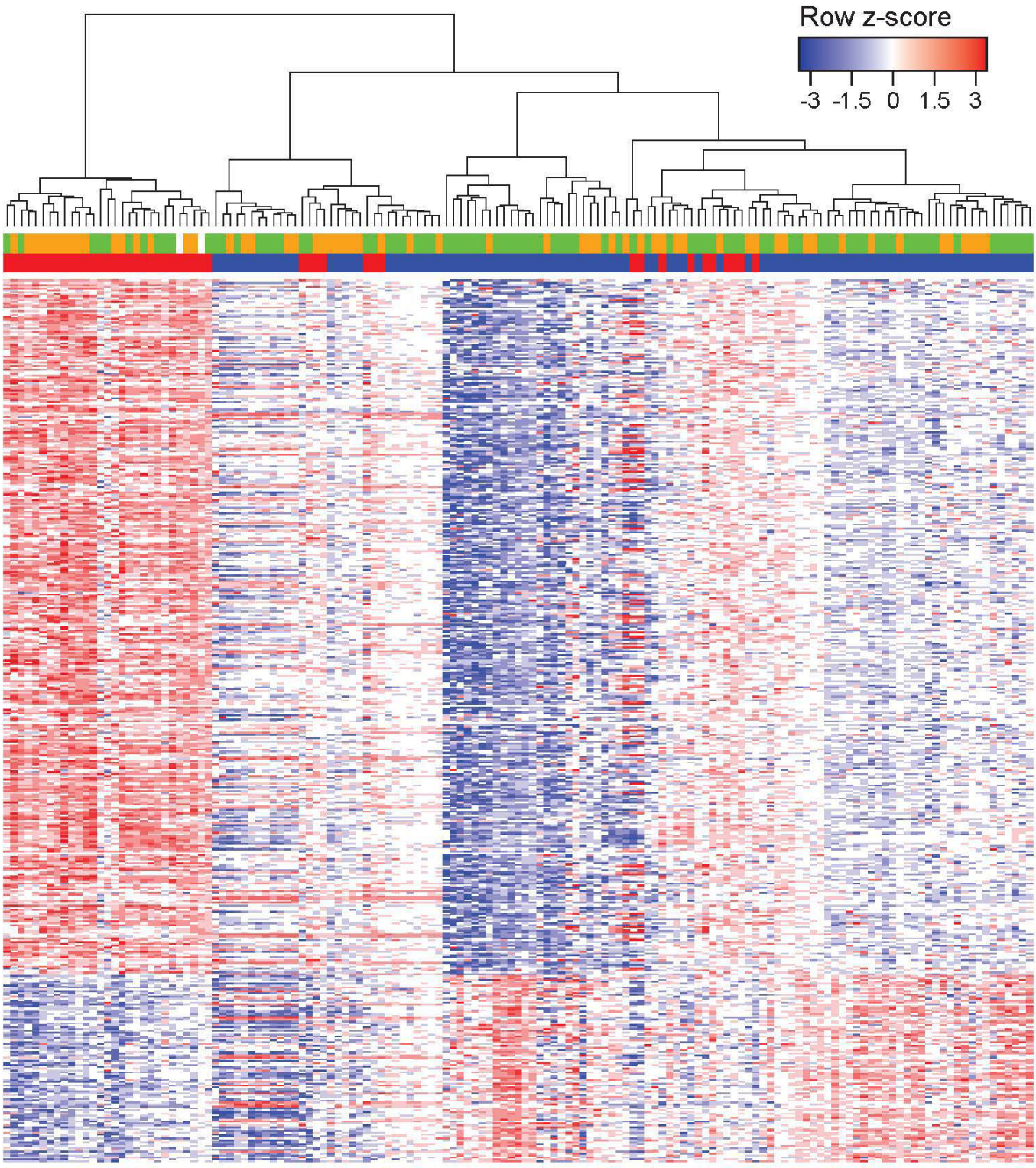

Figure 1a

Figure 1b

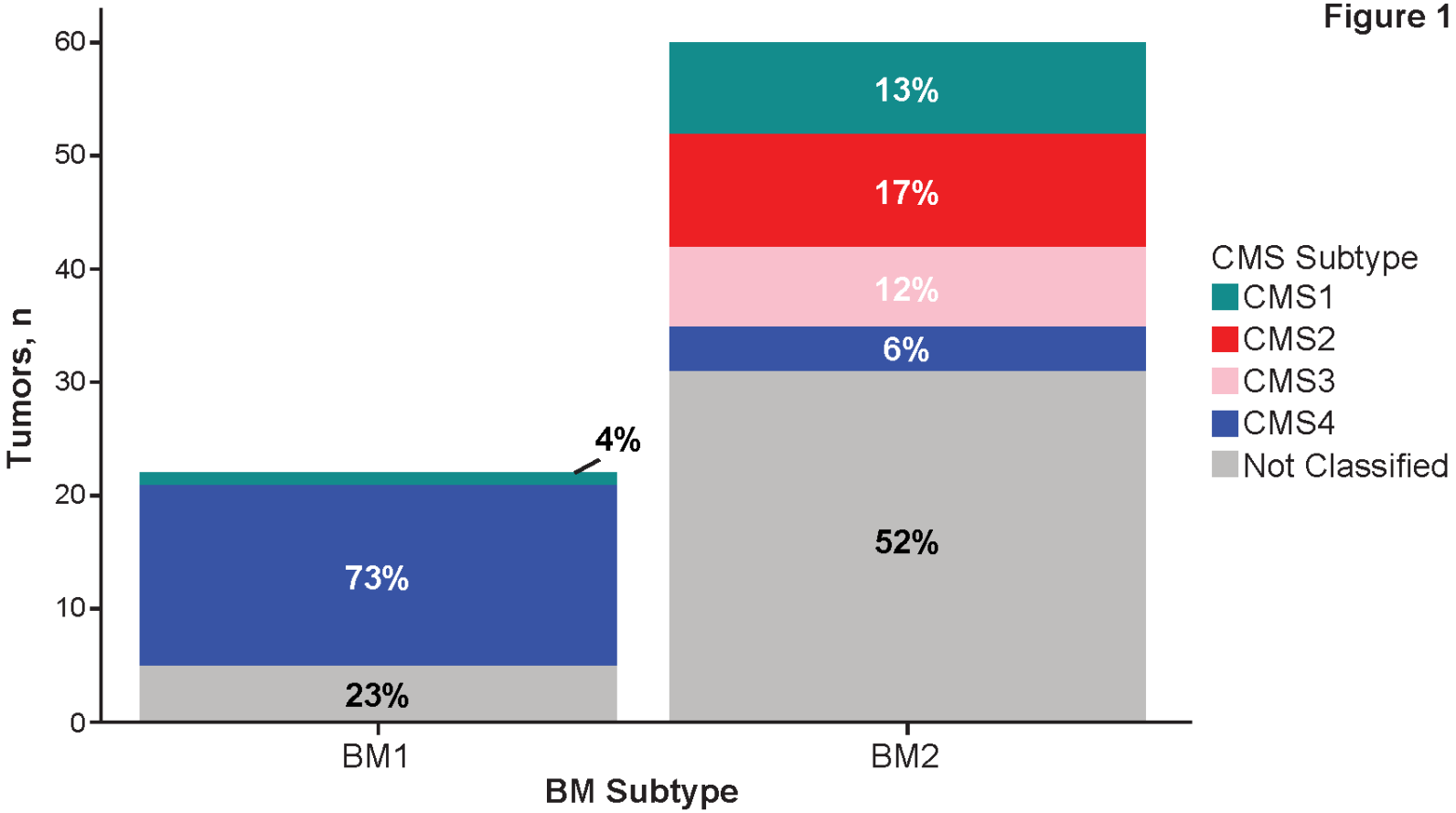

Figure 2

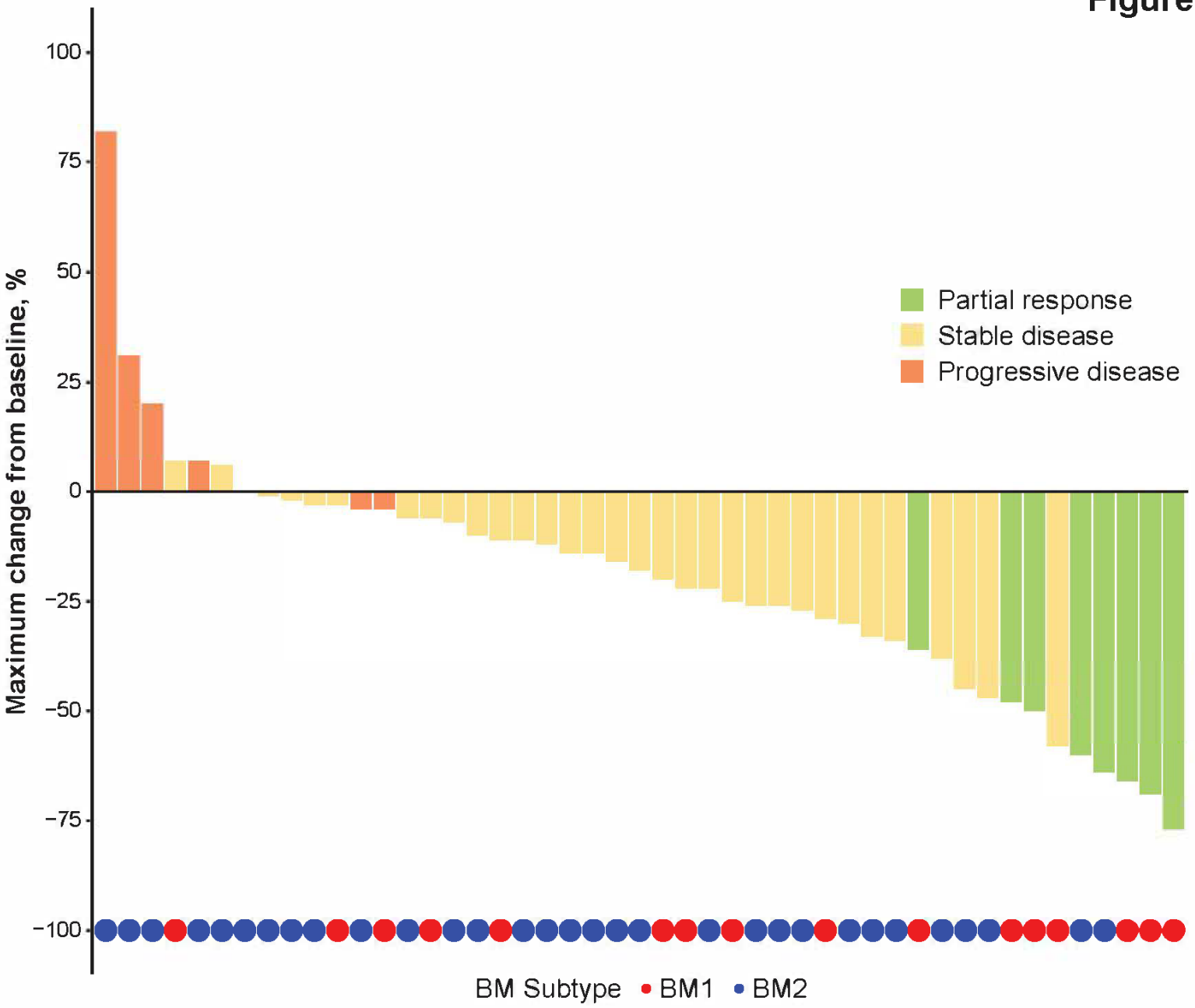

Figure 3a

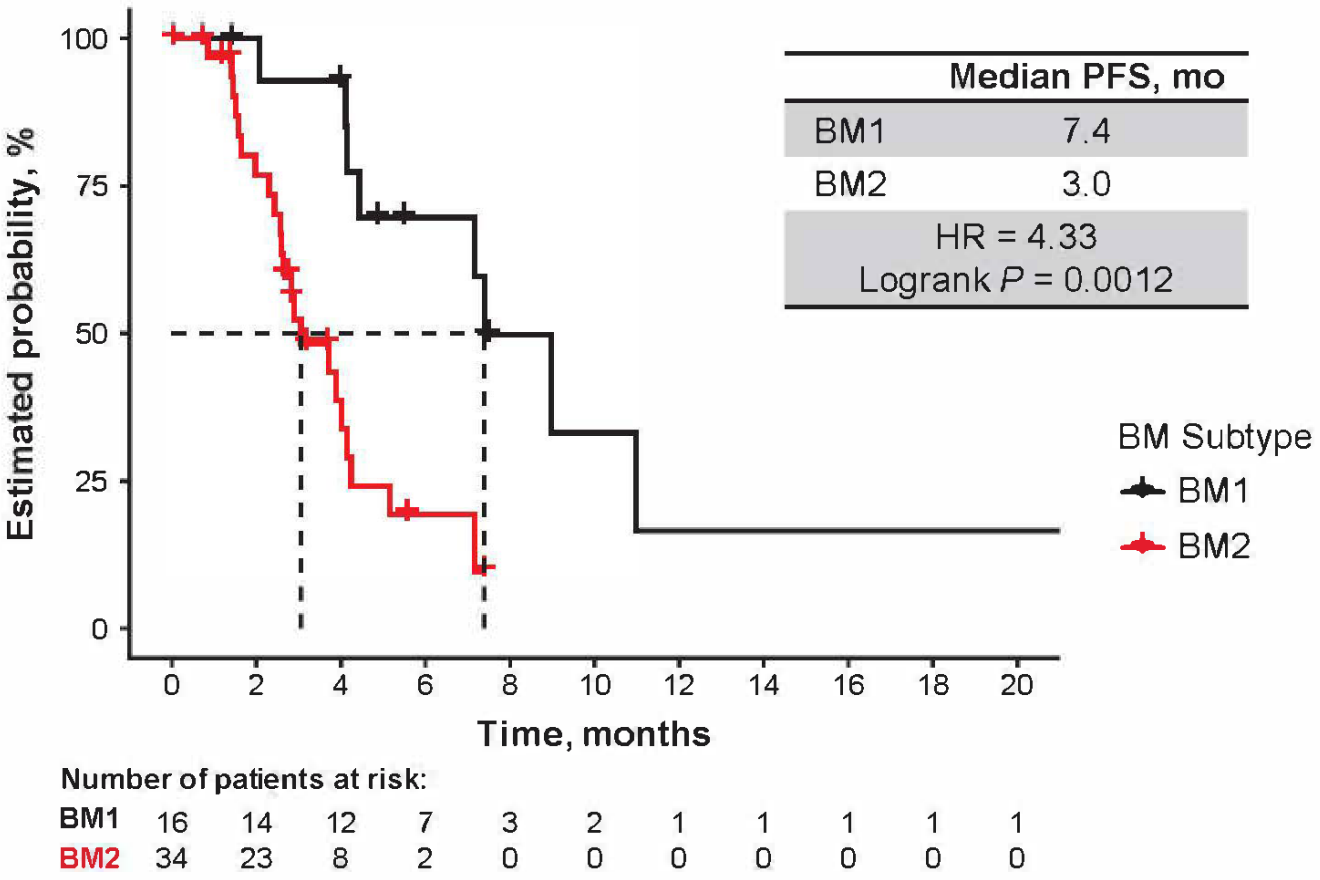

Figure 3b

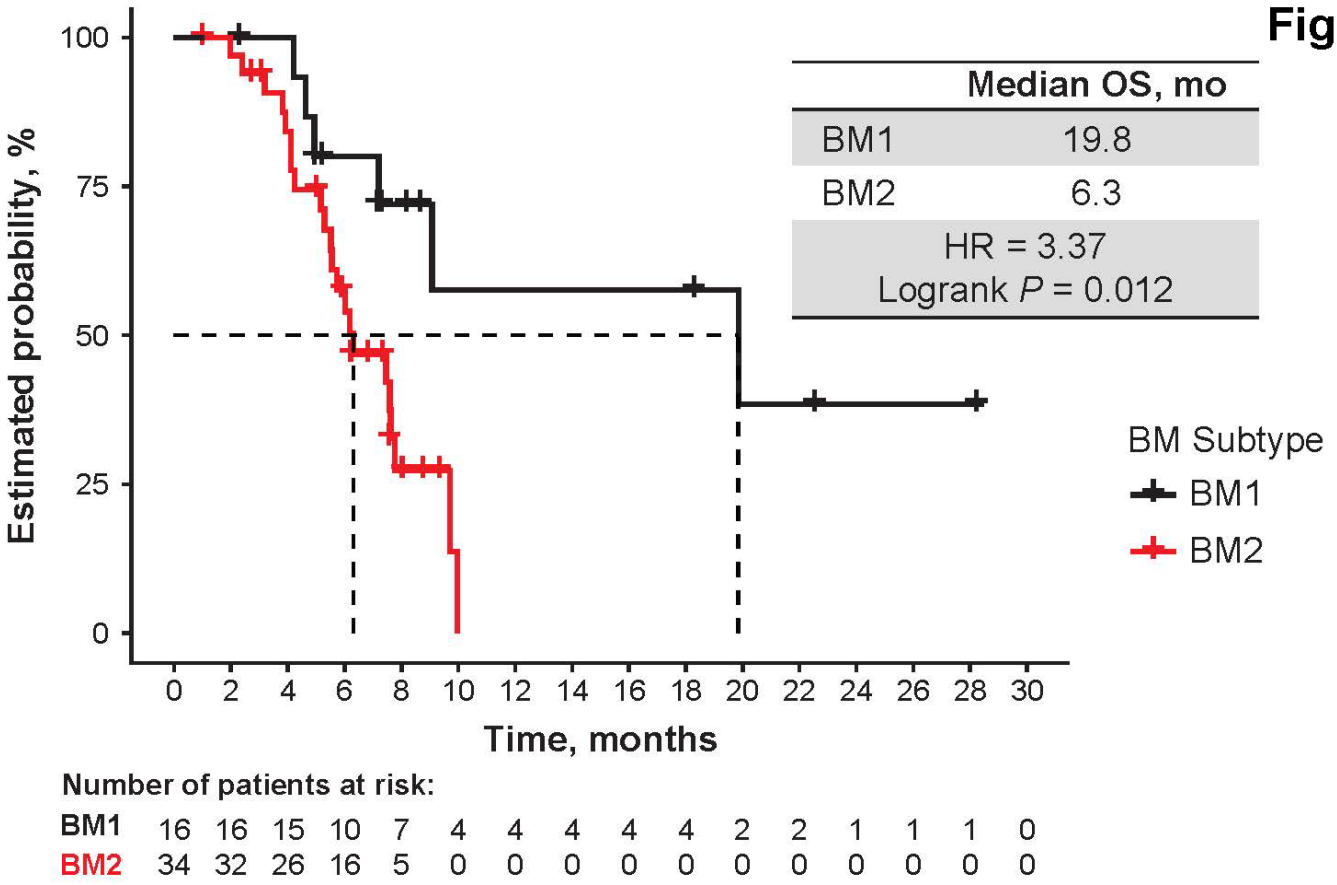

Figure 4

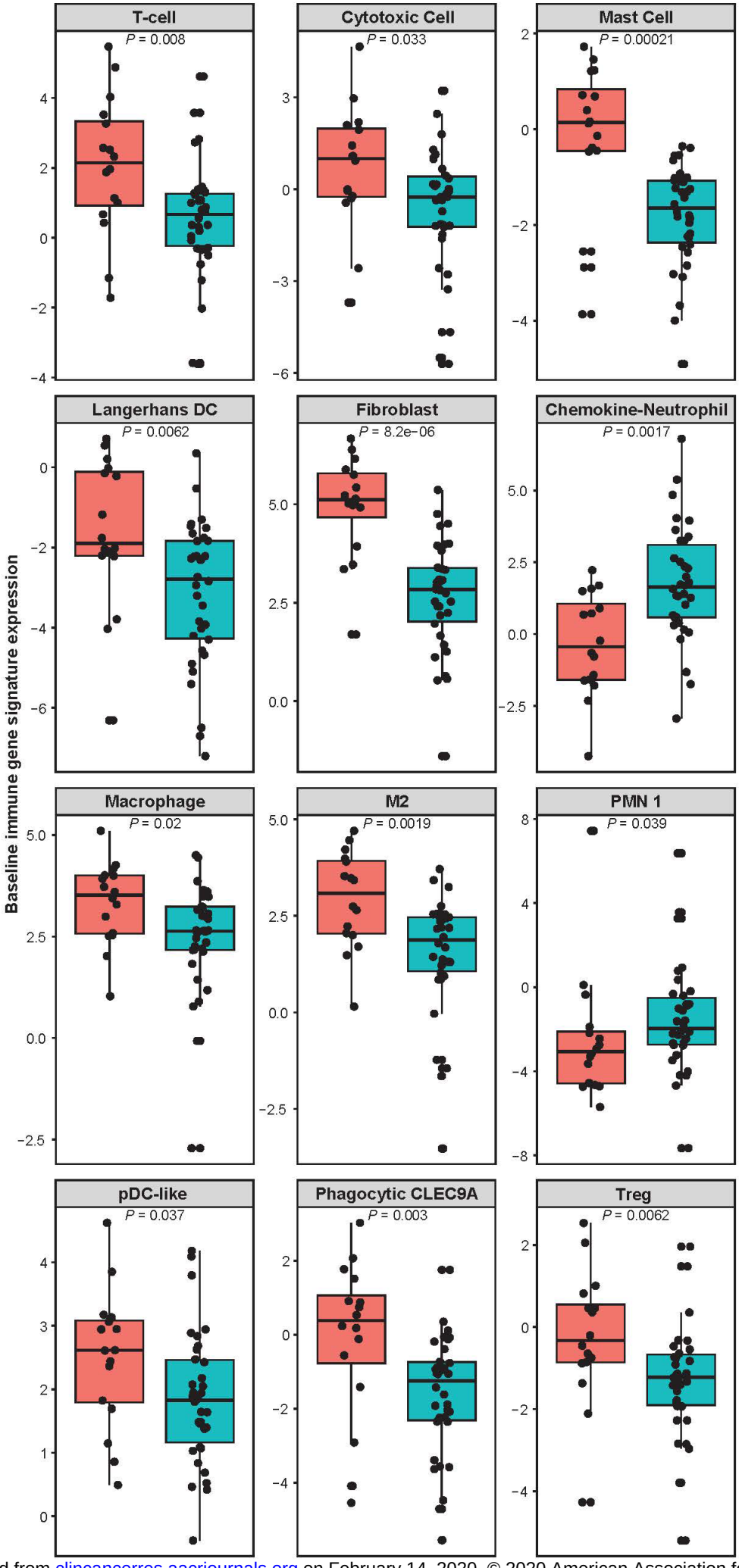

Figure 5

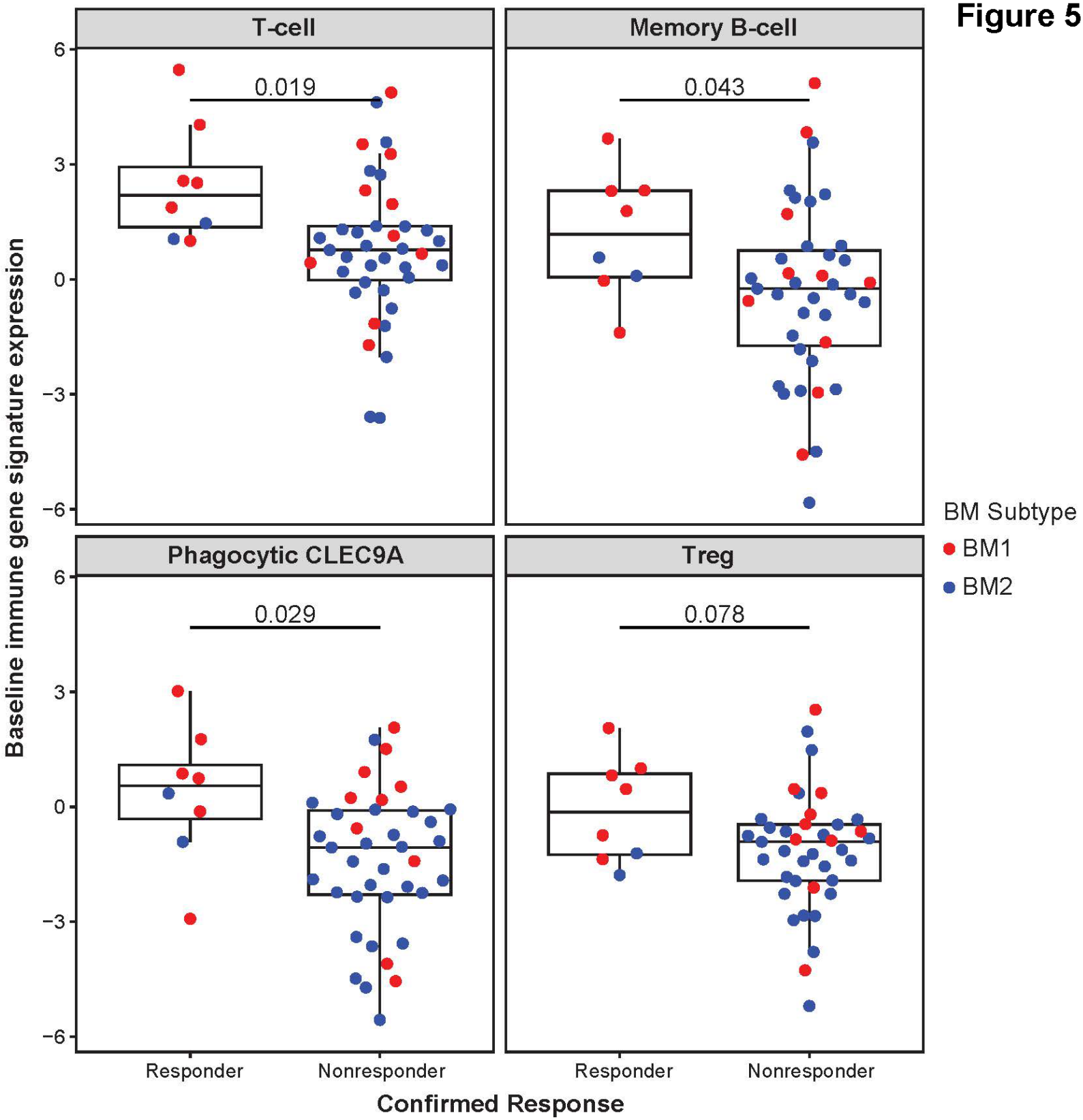

AACR American Association for Cancer Research

Clinical Cancer Research

BRAF-mutant Transcriptional Subtypes Predict Outcome of Combined BRAF, MEK, and EGFR Blockade with Dabrafenib, Trametinib, and Panitumumab in Patients with Colorectal Cancer

Gary Middleton, Yiqun Yang, Catarina D. Campbell, et al.

Clin Cancer Res Published OnlineFirst February 11, 2020.